Design and test of target-oriented profile modeling of unmanned aerial vehicle spraying

Peng Qi[1,2,3], Xiongkui He[1,2,3*], Yajia Liu[1,2,3], Yong Ma[4], Zhiming Wu[5], Jianwo Wang[6]

(1. *Centre for Chemicals Application Technology, China Agricultural University, Beijing 100193, China*;
2. *College of Science, China Agricultural University, Beijing 100193, China*;
3. *College of Agricultural Unmanned System, China Agricultural University, Beijing 101205, China*;
4. *Beijing Tianyi Hechuang Technology Development Co., Ltd., Beijing 100193, China*;
5. *Shanxi Agricultural University, Jinzhong 030801, Shanxi, China*;
6. *Hunan Crop Diseases and Pests Professional Control Association, Changsha 410015, China*)

Abstract: Unmanned aerial vehicles (UAVs) are a new frontier in specialized plant protection equipment, which will increasingly be utilized in modern sustainable agricultural applications. The use of UAVs retrofitted with new structures for spraying allows precision pesticide applications on fruit canopies, which have positive effects on pesticide reduction, along with fruit quality and production improvement. In this work, a precision toward-target device (BUAV) was established through profiling of fruit branch modeling, along with a quality analysis of the coverage in a pear orchard compared to a conventional multi-rotor UAV (CUAV). Coverage under different canopy sections and on both sides of leaves was evaluated using Polyvinyl Chloride card samplers. The results indicate that coverage of the BUAV was 0.98% and 1.41% on the abaxial of the lower leaves interior of the canopy, which was 2.38 and 3.14 times higher than that of the CUAV. The BUAV tended to increase coverage in the course-parallel direction, while both the course-parallel and vertical directions increased the deposition coverage on the abaxial side of the interior canopy leaves by 1.8 times and 2.1 times compared to the CUAV, respectively. Simultaneously, the BUAV increased the proportion of droplets deposited on the canopy and reduced ground loss. The BUAV can improve the distribution of the wind field within the canopy effectively and improve the droplet deposition on the reverse side of the interior bore blade.

Keywords: UAV, droplet coverage, target pesticide application, leaf abaxial side, profile spraying, orchard
DOI: 10.25165/j.ijabe.20221503.6753

Citation: Qi P, He X K, Liu Y J, Ma Y, Wu Z M, Wang J W. Design and test of target-oriented profile modeling of unmanned aerial vehicle spraying. Int J Agric & Biol Eng, 2022; 15(3): 85–91.

1 Introduction

Pears have an important production and trading position in the fruit industry of China, as the most widely planted fruit after apples and citrus, according to the Food and Agriculture Organization (FAO) of the United Nations and the State Statistics Bureau of China in 2019. In China, the pear tree cultivation area was up to 940.7 thousand hm^2, with a production of 17.3 million t, accounting for nearly 70% of the global output[1-3]. The utilization of chemical pesticides for pest control in pear orchards is very important. However, most pests and diseases occur upon the abaxial side of leaves, but it has been proven significantly difficult for conventional sprayers to reach the reverse side of the leaves. Long-duration excessive use of pesticides had led to increased resistance to pests and diseases[4-6]. In addition, significant amounts of pesticides are scattered during the application process, which severely affects the quality of pears and the ecosystem[7-9]. To ensure pesticide efficiency, during the spraying of orchards, pesticide droplets need to penetrate the canopy interior and reach the abaxial of the leaves. Consequently, for hydraulic and hydro-pneumatic sprayers, an air-assisted system is utilized to utilize strong wind and air capacity, to transfer droplets through the canopy and reach the leaf abaxial.

Many types of research conducted with Truck-Mounted Spraying Machine pesticide applications have been carried out to improve droplet deposition within the canopy, in which the deposition effects of different sprayers were compared[10], the angle of the plumb line was rotated[11], a single airflow was divided into three airflow bundles[12] and the nozzle angles were adjusted[13]. Moreover, the angles of the deflector and nozzle were bent to match the spindle-shaped crown of the modern planting mode[14]. It would therefore prove useful if these good solutions were applied to drones, utilizing the wide range of excellent ideas for aerial platforms that would turn them into popular designs for unmanned aerial vehicles (UAVs). UAVs have become comparatively economical equipment for utilization in agriculture[15]. Zhang et al.[16] used orthogonal experiments for flight altitude, speed, and volume to demonstrate the significance of these factors. Li et al.[17] designed fitting curves according to different altitudes, speeds, and spray pressures of drones, through which a spray uniformity relationship model could be established to obtain the best operating parameters. Wang et al.[18] concluded that the coverage mainly

Received date: 2021-05-16 **Accepted date:** 2021-12-18
Biographies: Peng Qi, PhD candidate, research interest: precise pesticide application and intelligent agricultural vehicle, Email: qi-peng@139.com; **Yajia Liu**, PhD, Associate Professor, research interest: precise pesticide application and pesticide residue, Email: liuyajia@cau.edu.cn; **Yong Ma**, MS, Research Fellow, research interest: horticultural science and plant protection, Email: 462416065@qq.com; **Zhiming Wu**, MS, Associate Professor, research interest: unmanned aerial vehicle and intelligent agricultural equipment, Email: zhim_wu@163.com; **Jianwo Wang**, PhD, Senior Engineer, research interest: extension of plant protection technique and unmanned aerial vehicle application technology, Email: 1437658276@qq.com.
***Corresponding author: Xiongkui He**, PhD, Professor, research interest: precise pesticide application and intelligent agricultural. No.2, Yuanmingyuan West Road, Haidian District, Beijing 100193, China. Tel: +86-10-62731446, Email: xiongkui@cau.edu.cn.

affected the speed of the bottom layer and height within the middle and bottom layers. Liu et al.[19] reported that better deposition occurs at a flight height of 2 m, speed of 1 m/s, and of four nozzles with 90° crossing. Han et al.[20] demonstrated that the addition of adjuvants could increase coverage and deposition, which was conducive to the penetration of the top and bottom canopies.

Although extensive interest exists in the positive significance of UAVs in agriculture, the instruments and constructions of aerial platforms have remained unchanged in recent years. These were based on existing UAV structures, without significant consideration of drones' structural evolution. Based on this consideration, an innovative application-specific structure was conceived to improve pesticide application using aerial platforms. A novel platform was first mounted on an unmanned aerial vehicle for profiling, modeling, and spraying of fruit branches. A comparison of these conventional UAVs with coverage as the evaluation index[21] would amplify the characteristics of droplet deposition, to provide a scientific basis for precision pesticide spraying applications.

2 Materials and methods

2.1 Development of BUAV

To realize a new spraying structure, the aerial platform model was utilized for the corresponding autonomous or semi-autonomous navigation and variable accurate volume application. The precision toward-target device (BUAV) was jointly developed by the Center for Chemicals Application Technology of China Agricultural University and Beijing Tianyi Hechuang Technology Development Co., Ltd.

Six-rotor unmanned aerial vehicle, which was widely adopted in the field of plant protection. In the study, a new system with toward-target spray and precision application technology was built on this UAV. A three-dimensional model of the UAV structure was designed using Unigraphics NX software (Figure 1). The primary parameters are listed in Table 1.

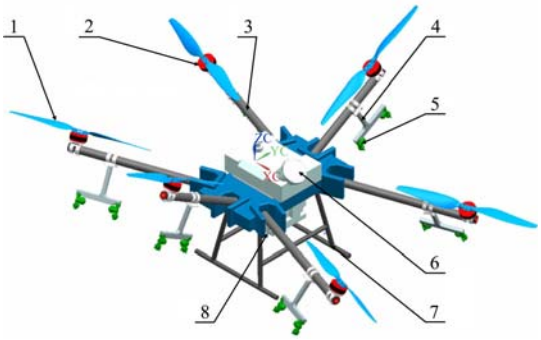

1. Rotor 2. Motor 3. Arm 4. Nozzle bracket 5. Nozzle 6. Tank 7. Undercarriage 8. Pump

Figure 1 3D model of the BUAV

Table 1 Main technical parameters of UAVs

Name	Parameters
Maximum flight speed	7 m/s
Dimensions	2509×2213×732 mm
Diameter × pitch	83.82 cm×22.86 cm (33 inch×9 inch)
Full tank volume	20 L
Nozzle model	SX11001/015VS
Maximum spray flow	3.6 L/min
Droplet size	130-250 μm
Flow range	0.25-20 L/min
Flow error	< (±2)%

The study made a structure transformation based on traditional UAVs. First, both the front and rear arms along the flight direction turned outwards (*Y*-axis), and the rotor and nozzle turned synchronously, as shown in Figures 2a and 2b. Second, the arms on the left and right sides of the UAV rotated upwards (*Z*-axis), and the rotor and nozzles did not rotate, as shown in Figures 2c and 2d.

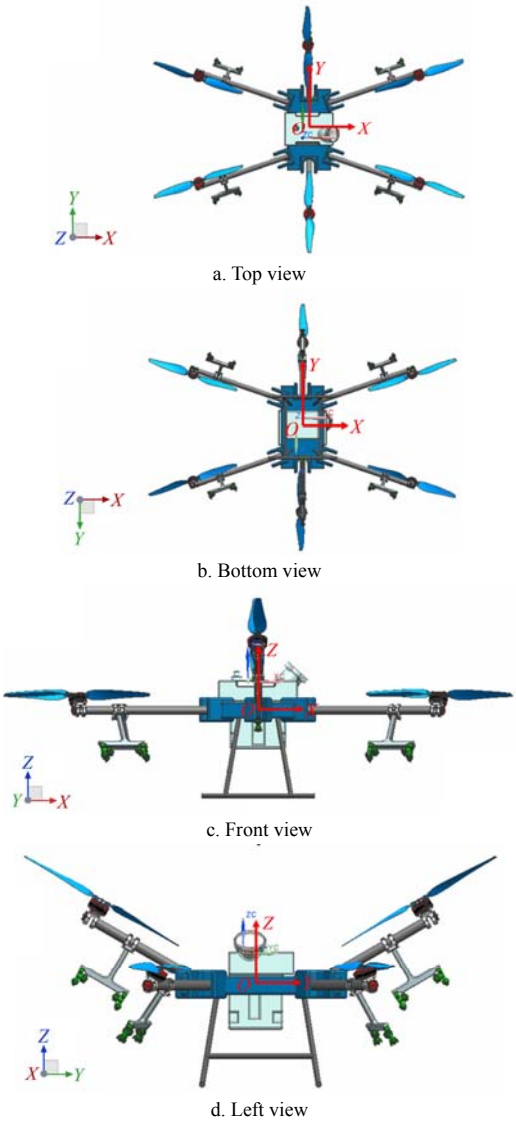

a. Top view

b. Bottom view

c. Front view

d. Left view

Figure 2 Different view of BUAV

In the top view of the BUAV, the numbers of the arms were defined as A1, A2, A3, A4, A5, A6, and the corresponding circular arrows were the direction of rotation. The angle between A3 and A4 in the forearm of the BUAV flight platform was 54°, and the angle between the rear arms was 56°. The arms A2 and A5 were perpendicular to the *X*-axis and parallel to the YZ plane. The reverse propeller was adapted on the A1, A4, and A5, while forward propeller was adapted on A2, A3, and A6 (Figure 3).

The fixed points of the A2 and A5 arms were separated by 470 mm, and on the same horizontal plane as the A1, A3, A5, and A6 arms. These two arms rotated 30° in the positive direction of *Z*-axis in the *YZ* plane around the fixed point (as shown in Figure 4).

In order to reach a relatively wide wind field spread, the arm of A4 and A6 had been rotated 30° counterclockwise around the center of the axis. In contrast, the arms of A1 and A3 arms had been rotated clockwise (Figure 5).

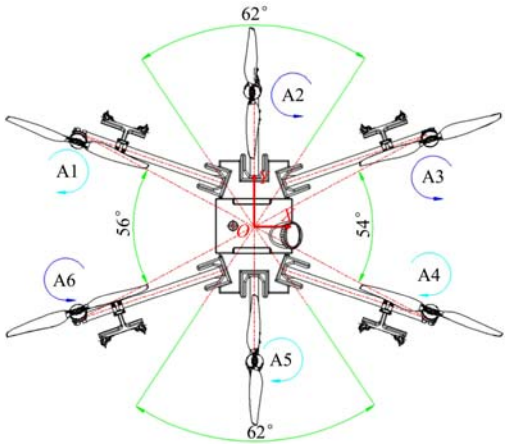

Figure 3 Arms angle and rotor direction in top view

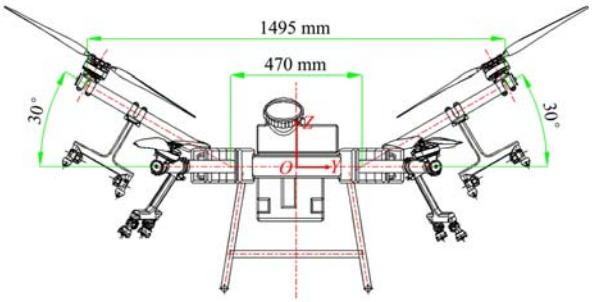

Figure 4 Arms angle of the left and right sides of the BUAV

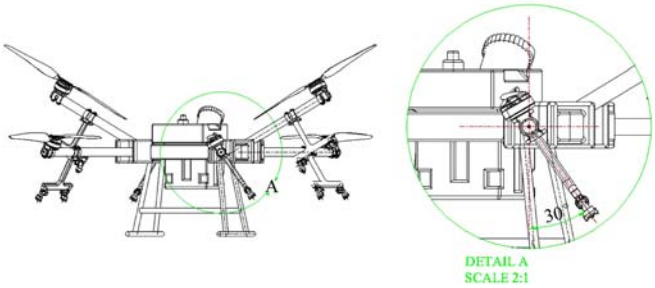

Figure 5 Partial schematic diagram of A6 arm

A new spray system was designed and constructed on the BUAV, which consisted of four components: eight brackets with two nozzles of each, a tank to store the pesticide, two diaphragm pumps, and automatic control spray activation. The horizontal distance between the bracket and the rotor was 205 mm, the distance between the nozzles and the fixed point of the bracket was 247 mm, the horizontal distances between the two nozzles and the rotor were 77 mm and 295 mm respectively (as shown in Figure 6).

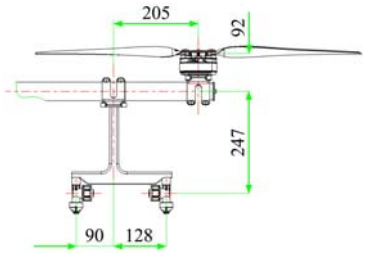

Figure 6 Bracket installation diagram

For the purposes of the present study, the T20 as a conventional multi-rotor UAV (CUAV) was used for comparison. This UAV had eight nozzles, distributed under the four rotors at the front and rear. The spray direction of the nozzle was vertically downward, all rotors of the CUAV had no rotation angle and pointed vertically downward.

The other specifications were of BUAV and CUAV were identical. The tank was located at the center of the sprayer, with a capacity of 20 L, an electric pump that applied a maximum pressure of 3 bar and operated at 12 V, while the integrated navigation and autopilot system provided autonomous control throughout the flight route.

2.2 Field experiments

2.2.1 Experimental site

To analyze the influence of the BUAV on spray distribution Field testing was carried out at the Pear Tree Test Field of the Fruit Tree Research Institute of Shanxi Academy of Agricultural Sciences, Taigu County, Jinzhong City, Shanxi Province, China (Latitude, 37°17'29.6", Longitude, 112°35'48.7"). The pear cultivation pattern followed a centerless trunk form – a modified cup shape. The pear trees were twenty-six years old. Also, they were 4.5 m in height and spaced at 3 m with a 4 m row separation, while the sizes of the canopies were approximately 4.0-4.5 m.

2.2.2 Section classification and collector arrangement

Three representative pear trees were randomly selected from a row of trees as the sampling area in the pear orchard. Each tree's canopy was divided into 32 zones, four height levels (ground, bottom, middle and top) (Figure 7a), as well as two radial depths (interior and exterior) (Figure 7b).

The front view was across the row, while the middle layer was 2.5 m above the ground. Also, the top and bottom layers were symmetrical to the middle layer, while the vertical intervals among these were 1m. The interior (circular solid line) and exterior (circular dashed line) canopies were 1 m and 1.5 m from the center, respectively. The top view of each tree was divided into four directions relative to the UAV's forward direction, denoted as front, back, left, and right.

Three leaves were randomly selected in each sampling section. A 24 mm×70 mm rectangular polyvinyl chloride card (PC) (Shanghai Hongshou Rubber Technology Center Co., Ltd., China) was used as a droplet collector, placed along the petiole, and fixed on the adaxial and abaxial of the leaf using a paperclip. The ground sampling areas were fixed on the ground with a paperclip; all sampling points were marked with red ribbons.

In this study, the test-paper method was used to measure the droplet deposition characteristics. The percentage of droplet coverage was used to measure the droplet deposition at the sampling points, and the coefficient of variation was used to determine the uniformity of droplet distribution in the field. The calculation equation of coverage percentage was as follows:

$$C = \frac{A_S}{A_P} \times 100\% \quad (1)$$

where, C represents the spray coverage percentage, %; A_s represents the number of pixels in the fog drop area; A_p represents the total number of pixels in the test strip area.

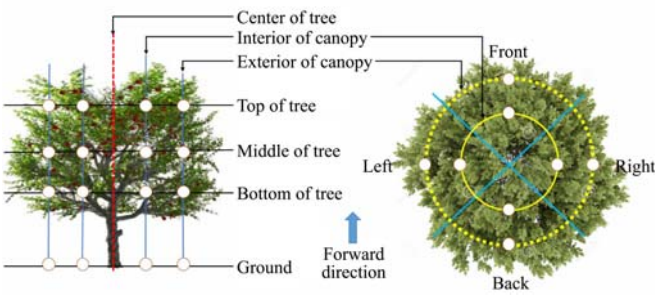

a. Front view b. Top view

Figure 7 Illustration of droplet collector arrangement at pear orchard

2.2.3 Spray applications

The field test was conducted in-between June 4-6, 2020 at the above-mentioned pear orchard. During the trial period, weather conditions were monitored at 1-hour intervals with the precision handheld Pocketwind IV anemometer Lechler GmbH· Agricultural Nozzles and Accessories, Germany. Moreover, the orchard conditions were: temperature of 22°C-26°C, the humidity of 60%-70%, and the wind speed of 1-2 m/s.

Before each application, the UAV tank was filled with clean water, which was then sprayed under the simulated flight parameters. A measuring cylinder was used to receive the water flow from each nozzle and test the flow rate. We changed the flow rate of the nozzles by adjusting the speed of the diaphragm pump to ensure that the total flow rate of the UAV nozzles was 75 L/hm^2. The BUAV used SX110015VS nozzles, with a working pressure of about 1.8 bar, and a flow rate of 0.45 L/min. The CUAV used SX11001VS nozzles, with a working pressure of 1.7bar and a flow rate of 0.3 L/min per nozzle. A water-based indicator Allure Red (Shanghai Dyestuff Research Institute Co., Ltd.) was used in all applications with a concentration of 30 g/L. For both drones, the speed was 2 m/s, the spray width was 4 m, the height from the ground was 5.0-5.5 m, the full load of the tank was 20 L and the rate of liquid spray was 75 L/hm^2. In addition, the flights were automatic with pre-set parameters. Due to the structural characteristics of the UAV, the BUAV atomization device sprayed obliquely downwards and the droplets entered the canopy along the direction of the branches, while the CUAV atomization device was pointed vertically downward, and the droplets were concentrated under the rotor. Therefore, the BUAV flew among the rows (Figure 8a), while the CUAV flew along the rows (Figure 8b). Both UAVs were operated in the direction of the arrow marked in Figure 9a. To reduce the impacts of UAV speed and droplets drift, the flights covered the entire sampling area (Figure 9b). Subsequently to spraying, when the droplet collectors were dried, the latter were marked and stored in ziploc bags under dry and dark conditions. Three replications per treatment were performed.

a. BUAV b. CUAV

Figure 8 UAV flight status during testing

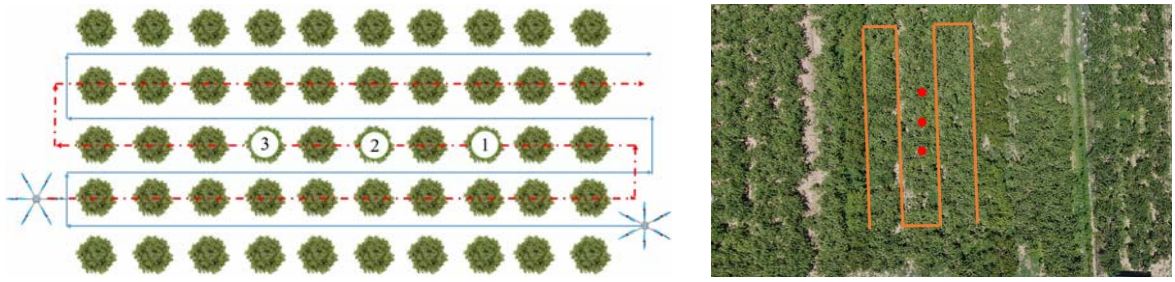

a. Diagram of flight pattern b. Flight area at pear orchard

Note: 1, 2, and 3 represent the sampling trees, respectively. The solid line is the flight trajectory of BUAV, while the dotted line is the flight trajectory of CUAV.

Figure 9 Schematic diagram of UAV operation course

2.3 Data analysis

Each PC was digitized with a camera (IXUS 105, Canon, Japan) and the image information was statistically obtained using the Deposit scan software (United States Department of Agriculture), to capture the percentage of coverage. The data were analyzed with Excel software (Microsoft Office 2016, Microsoft Corporation, Redmond, Washington, USA) and SPSS 22.0 (SPSS Inc, an IBM Company, Chicago, IL, USA) using the Duncan test at a significance level of 95%.

3 Results

3.1 Distribution of droplets on canopy between BUAV and CUAV

At the adaxial of pear leaves, the coverage efficiency of the BUAV was below that of the CUAV at the top, middle and bottom exterior canopy (Figure 10a), at 24.23%, 24.99%, 13.48%, respectively. Both had the highest coverage on the bottom layer, with a gradual decrease from bottom to top. The BUAV had 1.4 times higher coverage at the top interior canopy compared to the CUAV, while it had 27.27% lower coverage at the middle canopy (Figure 10b). Within the exterior and interior compartments, the mean coverage percentages of the BUAV and CUAV were 1.25%, 2.11% and 1.51%, 2.13%, respectively, which were 17.22% and 0.9% lower for the BUAV than the CUAV. Based on the univariate analysis of variance (Table 2) for the external and internal canopies, the differences were non-significant within groups and significant between groups.

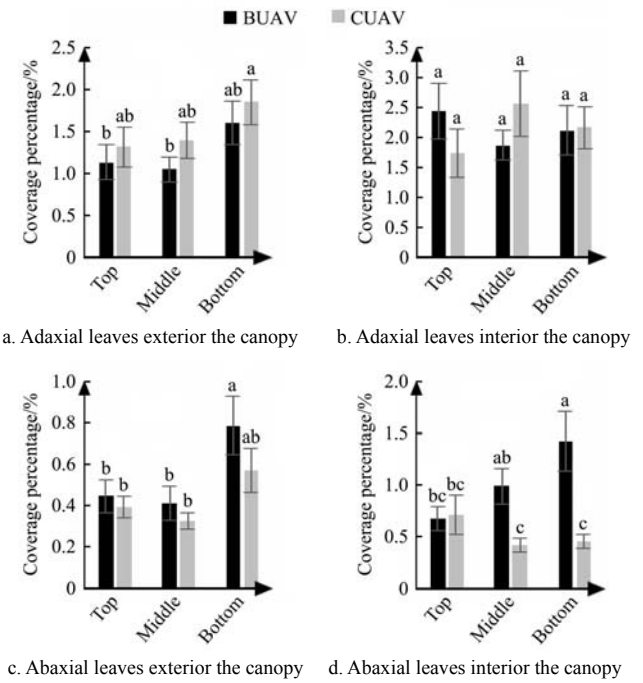

a. Adaxial leaves exterior the canopy b. Adaxial leaves interior the canopy

c. Abaxial leaves exterior the canopy d. Abaxial leaves interior the canopy

Figure 10 BUAV and CUAV distribution at canopies of fruit trees

Table 2 UAV Difference coverage percentage between exterior and interior canopies

Type	Canopy	Adaxial	Abaxial
BUAV	Exterior	1.25±0.12[b]	0.54±0.06[b]
	Interior	2.11±0.22[a]	1.02±0.12[a]
CUAV	Exterior	1.51±0.14[b]	0.42±0.04[b]
	Interior	2.13±0.25[a]	0.52±0.07[b]

Note: The average of the replicates is presented and with error bar mean ± standard error; different letters after data of the same index represent significant differences, while the same letters represent non-significant differences at the level of $p \leq 0.05$.

For the abaxial of pear leaves, the coverage efficiency of the BUAV was 1.14, 1.26, and 1.38 times higher than that of the CUAV, respectively, at the top, middle and lower layers of the exterior canopy (Figure 10c). The BUAV's coverage percentage was 4.88% lower than CUAV at the top interior canopy, but it was significantly higher at the middle and bottom layers by factors of 2.38 and 3.14, respectively (Figure 10d). As presented in Table 2, the coverage of the BUAV differed significantly from the other groups for the interior canopy, which confirmed that the BUAV significantly increased the coverage under side leaves for the interior canopy by a factor of 1.96 times, also following an increasing trend at the exterior canopy.

The results indicate that the coverage percentage of both types of UAV at the interior canopy was significantly higher than the exterior under the current test conditions. The BUAV significantly enhanced the coverage of abaxial leaves at the interior canopy, which significantly increased from top to bottom, whereas all other layers did not differ from the CUAV.

3.2 Distribution of droplets towards parallel and vertical directions of both UAVs

The main factors to consider were the distribution of droplets in the canopy, along with the front and rear directions of the pear tree, defined as the parallel directions of the route, while left and right were defined as the perpendicular directions of the route. These were compared and the UAV droplet distribution laws along the parallel and vertical directions of the course were analyzed.

On the adaxial of pear leaves, the BUAV had the lowest coverage of 0.83% for the exterior canopy along the vertical direction of the course (Figure 11), which was significantly lower than the path-parallel direction, but no differences existed compared to the CUAV. No significant differences existed between the parallel and vertical directions of the route at the interior canopy for the BUAV, which had increased coverage, but was significantly higher than the CUAV by a factor of 1.5 towards the vertical direction.

The CUAV had a maximum coverage of 2.56% towards the parallel direction of the interior canopy routes (Figure 12), which was significantly higher compared to the vertical direction of the canopy and the parallel direction of the exterior chamber for both UAVs.

Aimed at the reverse side of pear leaves, no differences existed between the two UAVs for the exterior canopy, while the BUAV had a significant advantage for the interior canopy. The BUAV coverage was significantly higher than the CUAV's by factors of 1.8 and 2.1 towards the parallel and vertical directions, also proving significantly higher by a factor of approximately 2 for the exterior canopy for both UAVs.

Results were obtained for the parallel and vertical directions of both UAVs. The two types of UAVs had a clear advantage on the adaxial side of the leaves at the interior canopy. No significant differences were found for the BUAV towards different directions of the course on the adaxial side of the leaves, while coverage tended to increase along the course-parallel direction. Significantly higher coverage was achieved by the BUAV at different positions on the course on the abaxial side of the interior canopy leaves.

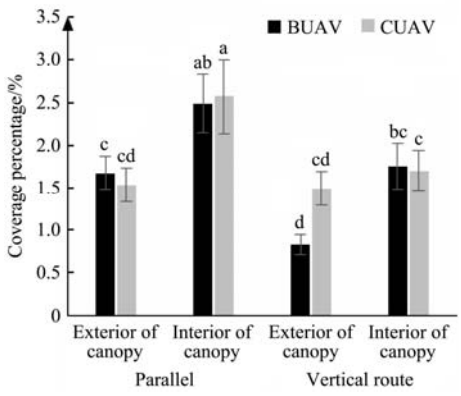

Figure 11 Coverage percentage of adaxial leaves for parallel and vertical routes

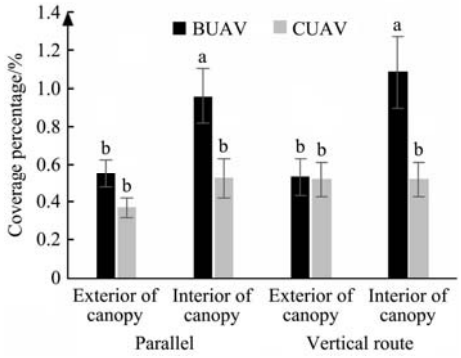

Figure 12 Coverage percentage of abaxial leaves for parallel and vertical routes

3.3 Droplet penetration analysis of both UAVs

The droplets moved throughout the pear canopy due to the downwash airflow of the drone, which was perpendicular from the top to the ground. The droplet collector on the adaxial leaves represented the penetration in the vertical direction of the canopy.

In the vertical direction of the exterior canopy (Figure 13a), the CUAV ground deposition coverage (2.48%) differed significantly from other locations, while no significant difference existed among layers. Along the vertical direction of the interior canopy (Figure 13b), no significant differences were observed among the sampling points.

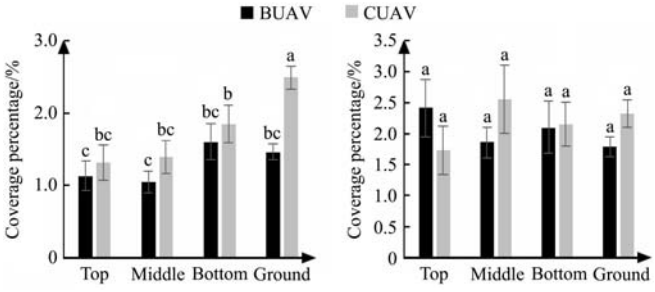

a. Exterior canopy b. Interior canopy

Figure 13 Both UAV penetration ratios

The results demonstrated that the BUAV increased the distribution ratio within the canopy and reduced the deposition of droplets on the ground. Simultaneously, the two types of UAVs penetrated the exterior canopy and reached the ground easily,

which occurred since the exterior canopy of the pear canopy had fewer leaves or was related to the ground effect.

4 Discussion

The initial wind field of the CUAV was concentrated directly under the fuselage[22], with the downwash flow demonstrating a tendency to contract and subsequently expand[23,24], as the wind field spread from the interior to the exterior of the canopy. The BUAV was above the exterior canopy. Consequently, the profiled structure promoted the direction angle of the droplet flow[25] so that it was directed to the target branch following the growth direction. The droplets were entrained in the wind field that moved towards the direction of the interior canopy, which caused the deposition on the interior to be significantly higher compared to the exterior canopy. Therefore, the interior canopy deposits of the two UAVs were significantly higher than the exterior canopy deposits.

Although the two UAVs followed similar laws on the adaxial leaves, the width of the wind field towards the parallel direction was significantly higher than the vertical direction[26,27]. Consequently, both parallel directions of the interior canopy demonstrated good deposition effects. The BUAV wind field moved to the interior of the canopy at a certain angle, reducing the interception of the top blades, easily turning the leaves, and increasing the chance of droplets meeting the blades, thereby forwarding the droplets' easy deposition on the reverse side of the leaves. This could explain the BUAV's higher coverage compared to CUAV.

When the drone was in operation, the stronger the downwash flow was, the more droplets were deposited in the effective spray range[28]. When the fruit trees were sprayed, the vertical downward air of the drone rotor occupied the dominant effect[29]. The fruit tree canopy had a significant blocking effect on the airflow under the rotor, while a vertical downward velocity stabilization zone no longer existed, which would cause velocity attenuation[30]. The CUAV wind field was mainly concentrated under the fuselage, while the downwash diffusion wind field[31] led the droplets to adhere to the fruit tree canopy under the influence of wind pressure. The wind field generated by the rotor blades was transmitted to the lower layers of the fruit trees and penetrated the canopy of pear trees to reach the ground. Due to the design structure of the profile, the wind field could be dispersed to a higher extent under the fuselage, which increased the width of the droplet distribution and prolonged the retention time interior of the canopy. Consequently, the proportion of deposition in the canopy was increased and the percentage of ground drift was reduced[32-34].

Also, problems with the BUAV occurred. Drone flight mainly relies on vertical upward force. Changing the UAV rotor structure increased energy consumption and affected the UAV's operational endurance to a certain extent. It was estimated that the corresponding endurance was reduced by 20%-30%. However, pests and diseases mainly occur on the abaxial of the leaves. Subsequently, the BUAV would have less opportunity to increase the deposition of droplets on the abaxial of the leaves, which could enhance the control effect of pests, as well as inspire the use of new equipment and methods for modern pear orchards. Furthermore, the BUAV wind field could entrain the droplet to move interior the complex canopy medium space. Finally, the droplet deposition laws still require further study.

5 Conclusions

Through this study, an orchard application technology based on profile modeling was proposed for the first time for the design and comparison of the BUAV and CUAV to research the droplet deposition regulation. Through the analysis of the droplet coverage, the interior, and exterior of the canopy, the top, middle and lower layers, along with the UAV towards the parallel and vertical directions of the route, the conclusions were: The interior canopy deposits of the two UAVs were significantly higher than the exterior canopy deposits. Compared to the CUAV, the BUAV had a significantly higher coverage of 1.96 times on the reverse side of the leaves interior the bottom interior canopy, which was at least 1.8 times higher towards both parallel and vertical directions along the course. Furthermore, both the CUAV and BUAV could improve the proportion of deposition interior the canopy and reduce the drift loss on the ground. This research provided new ideas for improving UAV applications in fruit management. Future studies will focus on exploring the different application effects with different UAV structures.

Acknowledgements

This work was financially supported by the National Key Research and Development Program of China (Grant No. 2020YFD1000202), Deutsche Forschungsgemeinschaft (DFG, German Research Foundation) 328017493/GRK 2366 (Sino-German International Research Training Group AMAIZE-P) and the National Modern Agricultural Industrial Technology System of China (Grant No. CARS-28-20). The authors also express their heartfelt gratitude to Wang Zhichong, Li Tian, Han Leng, Wang Changling, Huang Zhan, Xu Shaoqing, and the juniors of Shanxi Agricultural University.

[References]

[1] Food and Agriculture Organization of the United Nations Data-base (FAOSTAT). 2019. http://www.fao.org/faostat/en/#data/QCL Accessed on [2020-05-20]

[2] National Bureau of Statistics of China. Annual Data. http://data.stats.gov.cn/search.htm. Accessed on [2020-05-20]

[3] Zhang S L. Major problems facing the development of China's pear industry and countermeasures. China Fruit Industry, 2016; 33(12): 12–14. (in Chinese)

[4] Zhang S, Xie Z H. Current status, trends, main problems and the suggestions on development of pear industry in China. Journal of Fruit Science, 2019; 36(8): 1067–1072. (in Chinese)

[5] Tianna DuPont S, Strohm C, Nottingham L, Rendon D. Evaluation of an integrated pest management program for central Washington pear orchards. Biol Control, 2021; 152: 104390. doi: 10.1016/j.biocontrol.2020.104390.

[6] Li Z X, Nie J Y, Yan Z, Xu G F, Li H F, Kuang L X, et al. Risk assessment and ranking of pesticide residues in Chinese pears. J Integr Agric, 2015; 14(11): 2328–2339.

[7] He X K. Research progress and developmental recommendations on precision spraying technology and equipment in China. Smart Agriculture, 2020; 2(1): 133–146.

[8] Changling W, Xiongkui H, Jane B, Peng Q, Yi Y, Wanling G. Effect of downwash airflow field of 8-rotor unmanned aerial vehicle on spray deposition distribution characteristics under different flight parameters. Smart Agric, 2020; 2(4): 124–136.

[9] Wang X N, He X K, Wang C L, Wang Z C, Li L L, Wang S L, et al. Spray drift characteristics of fuel powered single-rotor UAV for plant protection. Transactions of the CSAE, 2017; 33(1): 117–123. (in Chinese)

[10] Sinha R, Ranjan R, Khot L R, Hoheisel G A, Grieshop M J. Comparison of within canopy deposition for a solid set canopy delivery system (SSCDS) and an axial–fan airblast sprayer in a vineyard. Crop Prot., 2020; 132: 105124. doi: 10.1016/J.CROPRO.2020.105124.

[11] Bahlol H Y, Chandel A K, Hoheisel G A, Khot L R. The smart spray analytical system: Developing understanding of output air-assist and spray patterns from orchard sprayers. Crop Prot., 2020; 127: 104977. doi: 10.1016/J.CROPRO.2019.104977.

[12] Lyu X L, Zhang M N, Chang Y H, Lei X H, Yang Q S. Influence of deflector angles for orchard air-assisted sprayer on 3D airflow distribution. Transactions of the CSAE, 2017; 33(15): 81–87. (in Chinese)
[13] Foqué D, Nuyttens D. Effects of nozzle type and spray angle on spray deposition in ivy pot plants. Pest Manag Sci., 2011; 67(2): 199–208.
[14] Bakker T, Wouters H, van Asselt K, Bontsema J, Tang L, Müller J, et al. A vision based row detection system for sugar beet. Computers and Electronics in Agriculture, 2008; 60(1): 87–95.
[15] He X K. Rapid development of unmanned aerial vehicles (UAV) for plant protection and application technology in China. Outlooks on Pest Manag., 2018; 29(4): 162–167.
[16] Zhang X Q, Song X P, Liang Y J, Qin Z Q, Zhang B Q, Wei J J, et al. Effects of spray parameters of drone on the droplet deposition in sugarcane canopy. Sugar Tech., 2020; 22(4): 583–588.
[17] Li J Y, Lan Y B, Zhou Z Y, Zeng S, Huang C, Yao W X, et al. Design and test of operation parameters for rice air broadcasting by unmanned aerial vehicle. Int J Agric & Biol Eng, 2016; 9(5): 24–32.
[18] Wang B J, Pan B, Jiang L, Lin Y, Zhao S, Mo Y X. Effects of spraying parameters of plant protection unmanned aerial vehicle on deposition distribution of droplets in pitaya canopy. Journal of Agricultural Science and Technology, 2020; 22(10): 101–109. (in Chinese)
[19] Liu Q, Lan Y B, Shan C F, Mao Y D. The influence of spraying parameters of aerial application on droplet deposition characteristics for apple fields. Journal of Agricultural Mechanization Research, 2020; 42(9): 173–180.
[20] Han P, Cui Z Y, Yan X J, Shi W P, Wang F L, Yuan H Z. Effect of three types of spray adjuvants on the distribution of spray droplet deposition in hilly citrus under precise fruit tree operation mode of unmanned aerial vehicles. Chinese Journal of Pesticide Science, 2020; 22(6): 1076–1084. (in Chinese)
[21] Salyani M, Fox R D. Evaluation of spray quality by oil and water-sensitive papers. Transactions of the ASAE, 1999; 42(1): 37–43.
[22] Baetens K, Nuyttens D, Verboven P, De Schampheleire M, Nicolaï B, Ramon H. Predicting drift from field spraying by means of a 3D computational fluid dynamics model. Computers and Electronics in Agriculture, 2007; 56(2): 161–173.
[23] Xu T Y, Yu F H, Cao Y, Du W, Ma M Y. Vertical distribution of spray droplet deposition of plant protection multi rotor UAV for Japonica rice. Transactions of the CSAM, 2017; 48(10): 101–107. (in Chinese)
[24] Kiran R, Ahmed R, Salehi S. Experiments and CFD modelling for two phase flow in a vertical annulus. Chem Eng Res Des, 2020; 153: 201–11.
[25] Zhang H, Qi L, Wu Y, Musiu E M, Cheng Z, Wang P. Numerical simulation of airflow field from a six–rotor plant protection drone using lattice Boltzmann method. Biosyst Eng., 2020; 197: 336–351.
[26] Li J Y, Zhou Z Y, Lan Y B, Hu L, Zang Y, Liu A M, et al. Distribution of canopy wind field produced by rotor unmanned aerial vehicle pollination operation. Transactions of the CSAE, 2015; 31(3): 77–86. (in Chinese)
[27] Li J Y, Zhou Z Y, Hu L, Zang Y, Xu S, Liu A M, et al. Optimization of operation parameters for supplementary pollination in hybrid rice breeding using round multi-axis multi-rotor electric unmanned helicopter. Transactions of the CSAE, 2014; 30(11): 1–9. (in Chinese)
[28] Tang Q, Zhang R R, Chen L P, Deng W, Xu M, Xu G, et al. Numerical simulation of the downwash flow field and droplet movement from an unmanned helicopter for crop spraying. Comput Electron Agric., 2020; 174: 105468. doi: 10.1016/j.compag.2020.105468.
[29] Zhang H, Qi L J, Wu Y L, Cheng Z Z, Liu W W, Musiu E, et al. Distribution characteristics of rotor downwash airflow field under spraying on orchard using unmanned aerial vehicle. Transactions of the CSAE, 2019; 35(18): 44–54. (in Chinese)
[30] Zhang H, Qi L J, Wu Y L, Liu W W, Cheng Z Z, Musiu E. Spatio-temporal distribution of down-wash airflow for multi-rotor plant protection UAV based on porous model. Transactions of the CSAM, 2019; 50(2): 112–122. (in Chinese)
[31] Yang Z L, Ge L Z, Qi L J, Cheng Y F, Wu Y L. Influence of UAV rotor down-wash airflow on spray width. Transactions of the CSAM, 2018; 49(1): 116–122. (in Chinese)
[32] Wang C L, He X K, Zeng A J. Measuring method and experiment on spray drift of chemicals applied by UAV sprayer based on an artificial orchard test bench. Transactions of the CSAE, 2020; 36(13): 56–66. (in Chinese)
[33] Zhao H Y, Xie C, Liu F M, He X K, Zhang J, Song J L. Effects of sprayers and nozzles on spray drift and terminal residues of imidacloprid on wheat. Crop Prot, 2014; 60: 78–82.
[34] Herbst A, Bonds J, Wang Z C, Zeng A J, He X K, Goff P, et al. The influence of unmanned agricultural aircraft system design on spray drift. J fur Kult, 2020; 72(1): 1–11. doi: 10.5073/JfK.2020.01.01.